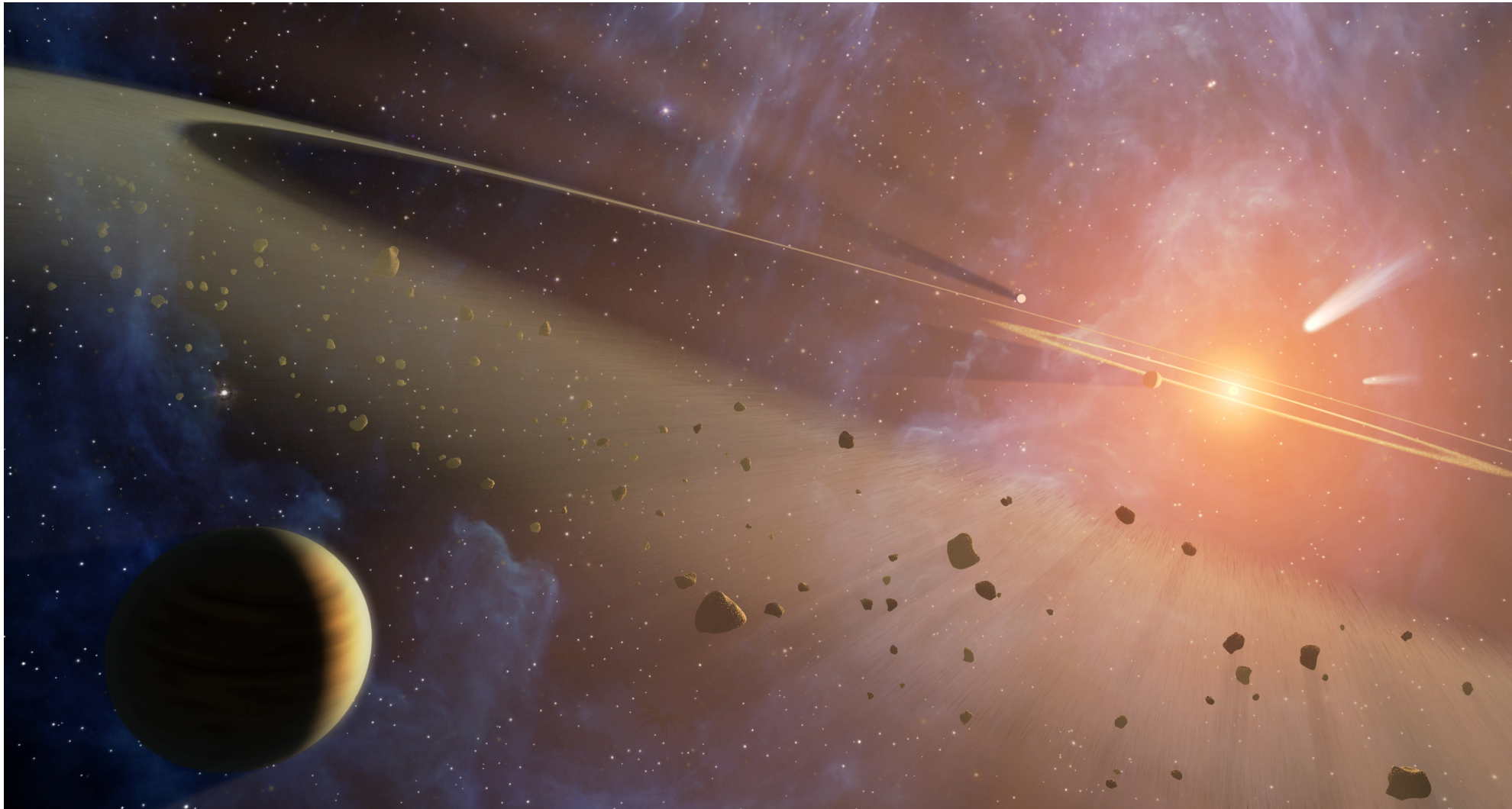


*Direct detection:
Seeking exoplanet colors and spectra*



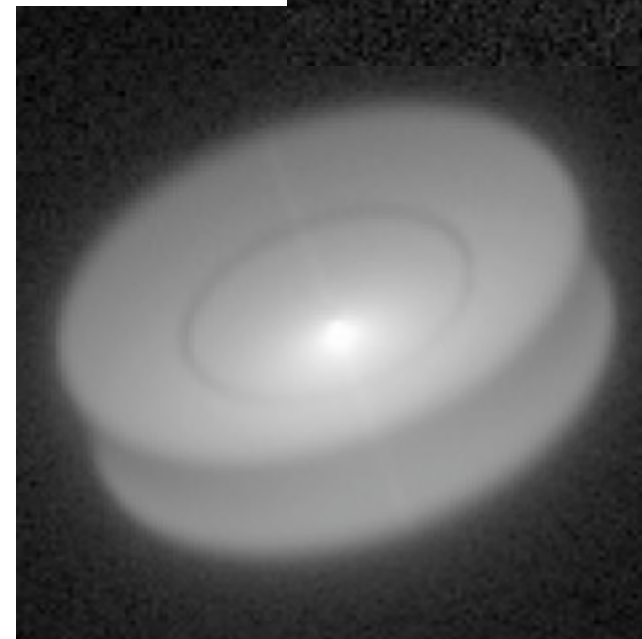
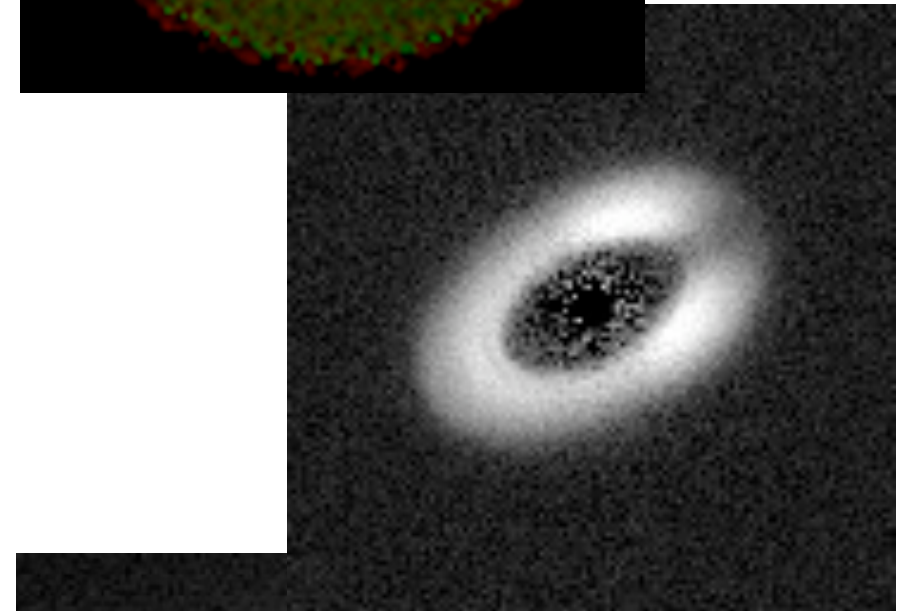
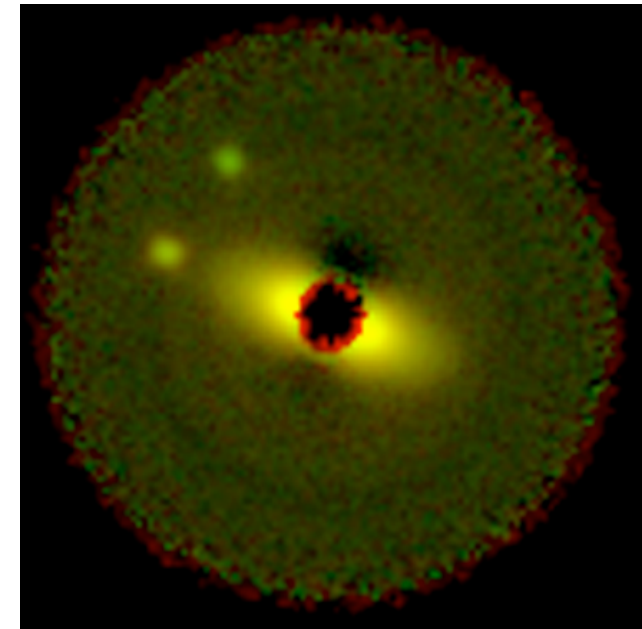
*John Trauger, JPL / Caltech
Keck Institute for Space Studies Workshop
Caltech -- 10 November 2009*

(c) 2009 California Institute of Technology. Government sponsorship acknowledged.

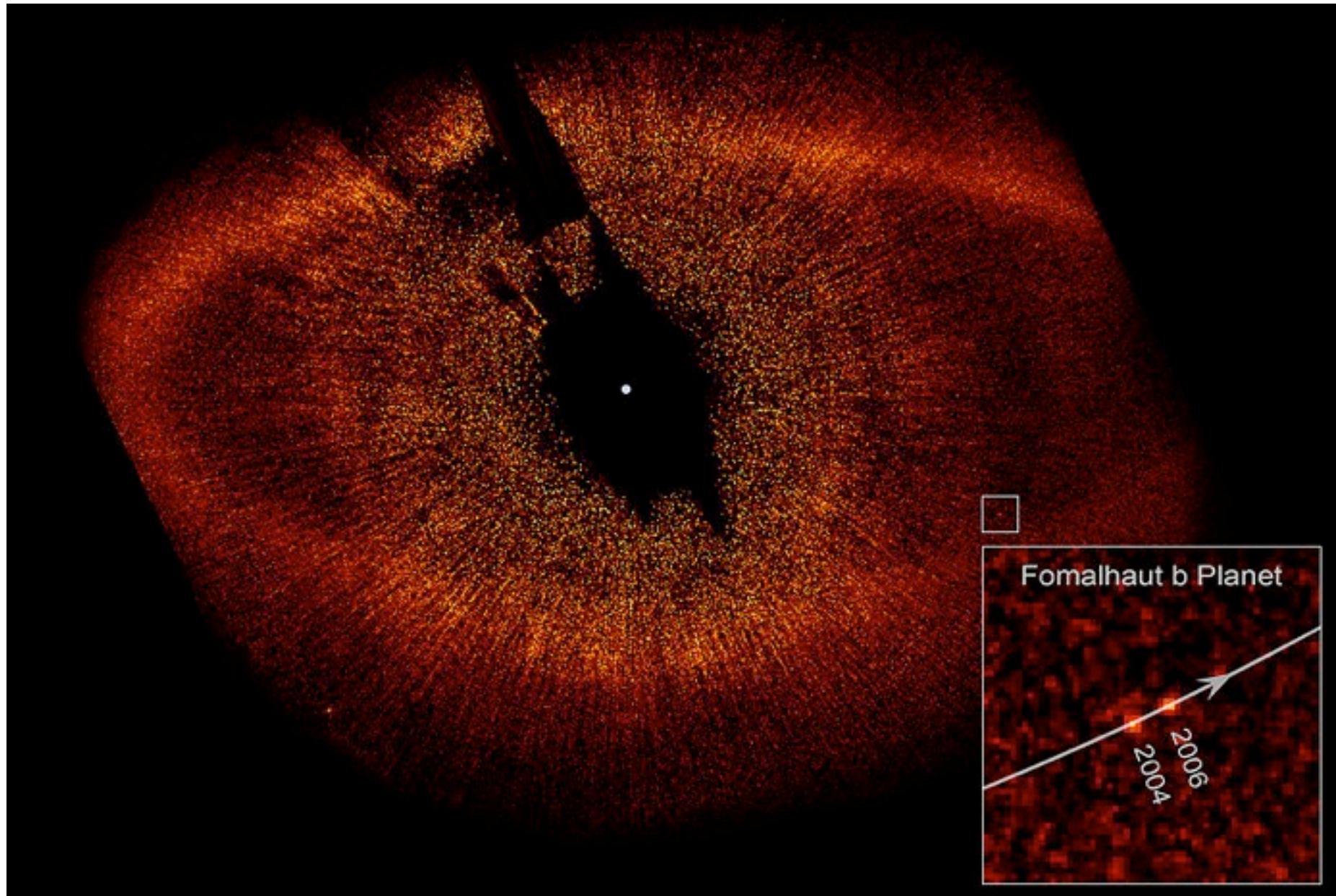
Science objectives

Exoplanetary systems, possibly dynamically full, that harbor exoplanets, planetesimals, dust structures.

- *Direct coronagraphic imaging and low-resolution spectroscopy of exoplanet systems in reflected starlight, to include:*
- *Census of nearby known RV planets in orbits beyond $\sim 1\text{AU}$*
- *Search for mature exoplanet systems beyond the RV survey limits, including giant planets, super-earths, and possibly a dozen earth-mass planets*
- *Dust structures as an indicator of unseen planets and planetesimals*
- *Dust structure in the circumstellar environment as a probe of the life cycle of planetary systems: from young stellar objects to proto-planetary nebulae*

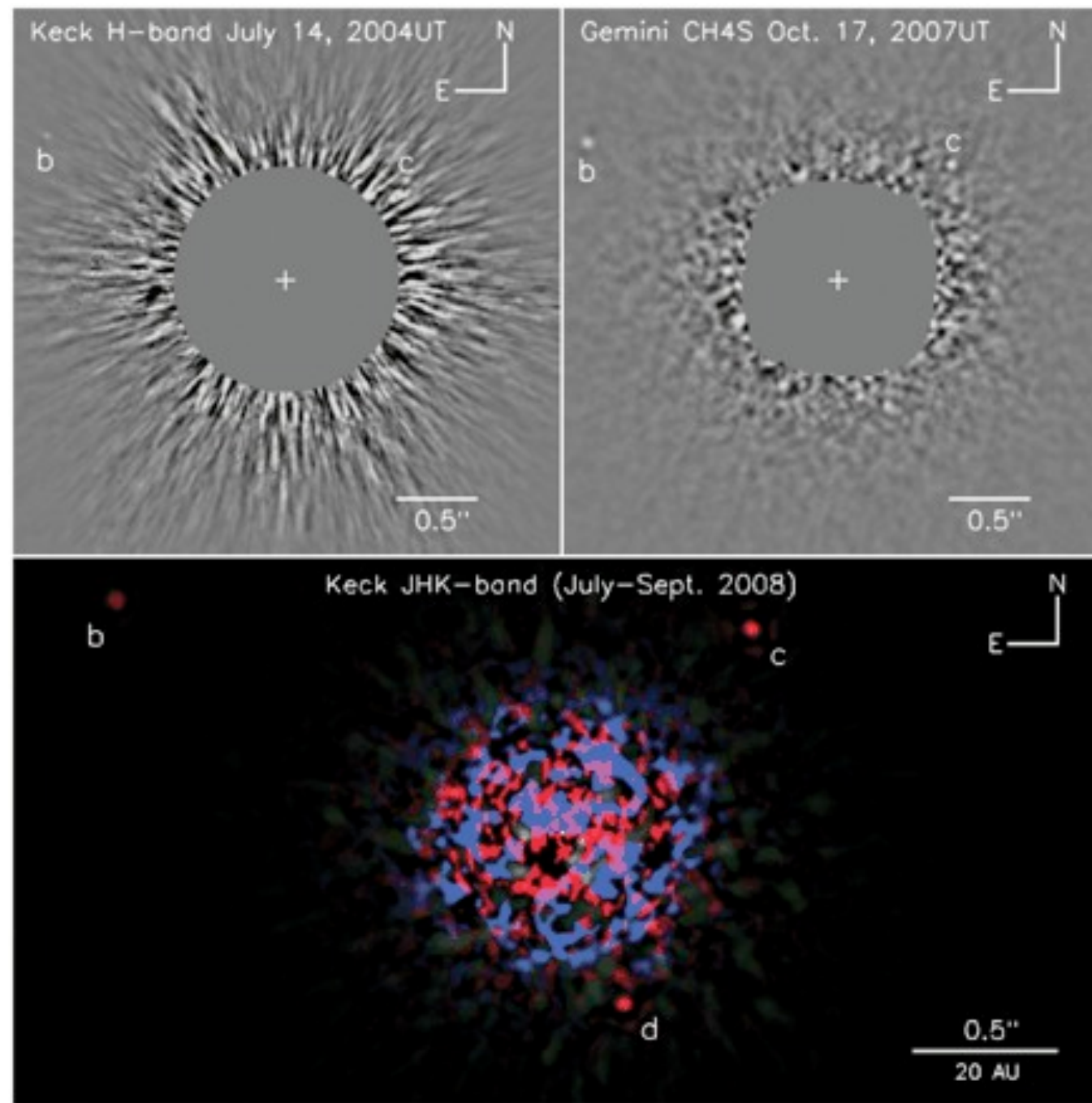


The first direct images!



(Kalas et al., Science 2008)

Hubble/ACS coronagraph image of a 0.5-3 Jovian mass exoplanet orbiting Fomalhaut. Inner clearing of the eccentric ring suggested the presence of an exoplanet, as confirmed in these direct images.



(Marois et al., NRC-HIA & Keck telescope, Science 2008)

Three planets orbiting HR8799. System is favorable for observation from ground-based observatories because the planets are large (~10 Jupiter masses), young (~60 million years), self-luminous (~100,000 times brighter than Jupiter), and three or more times further from the star than Saturn is from the Sun.

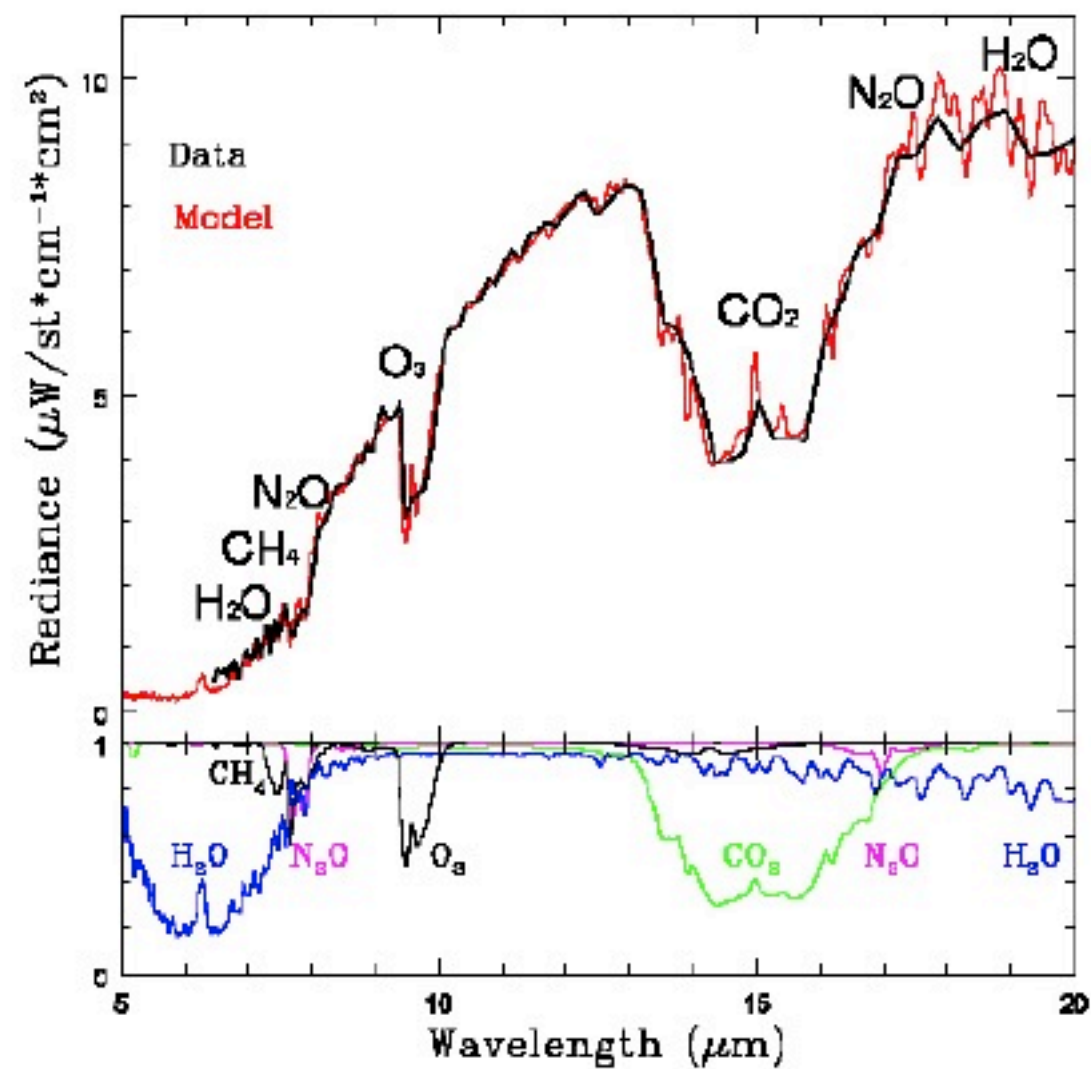
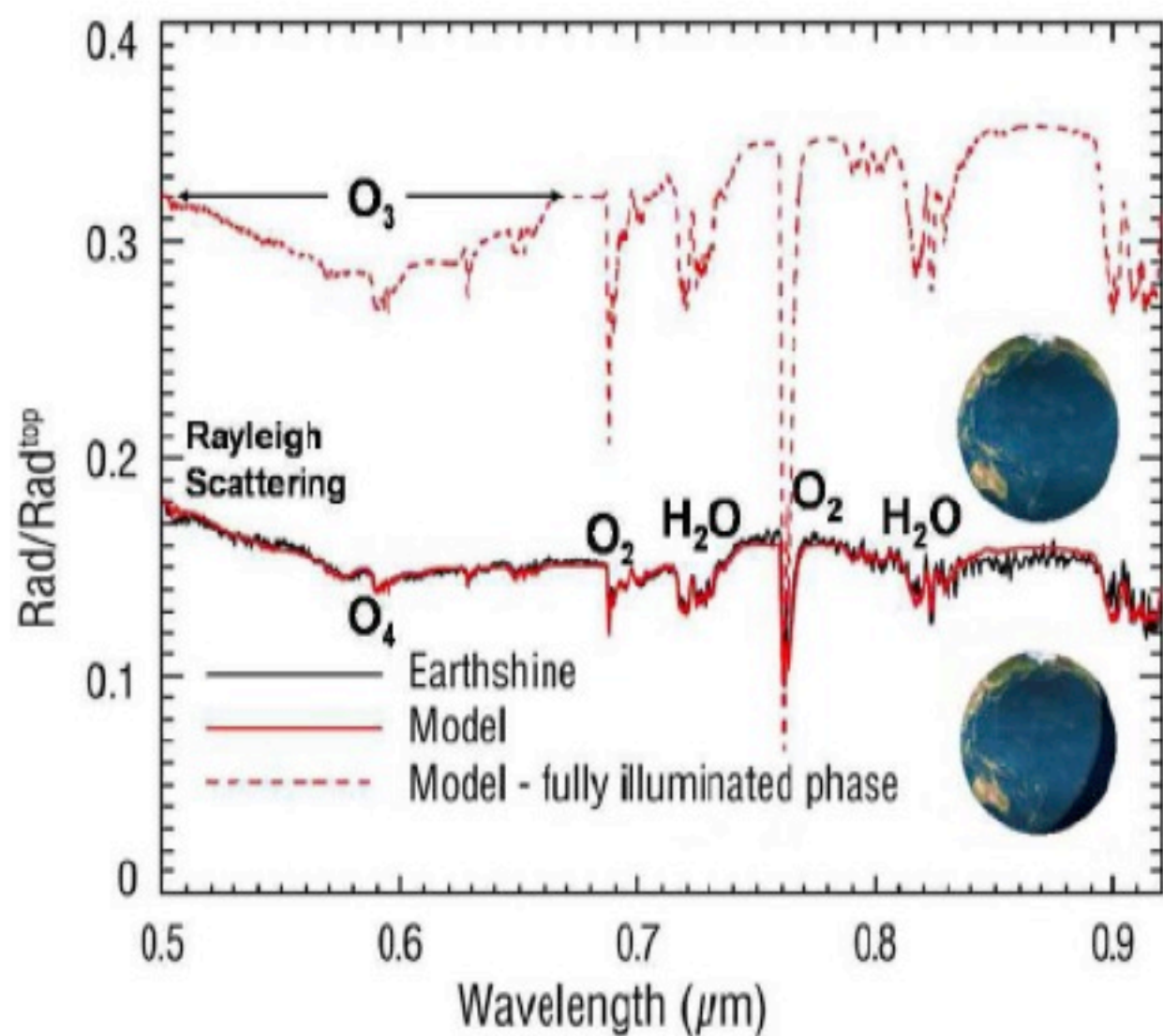
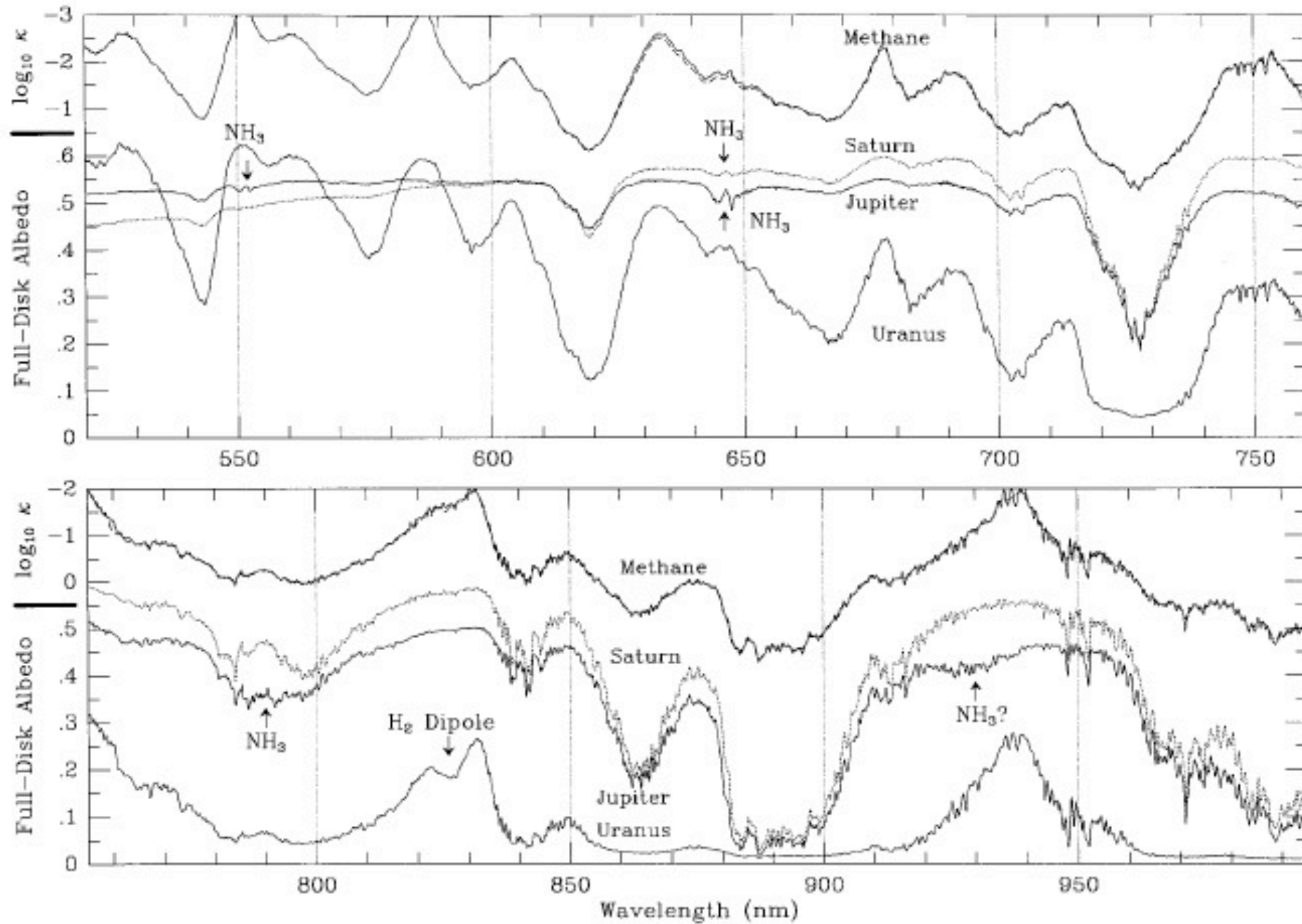
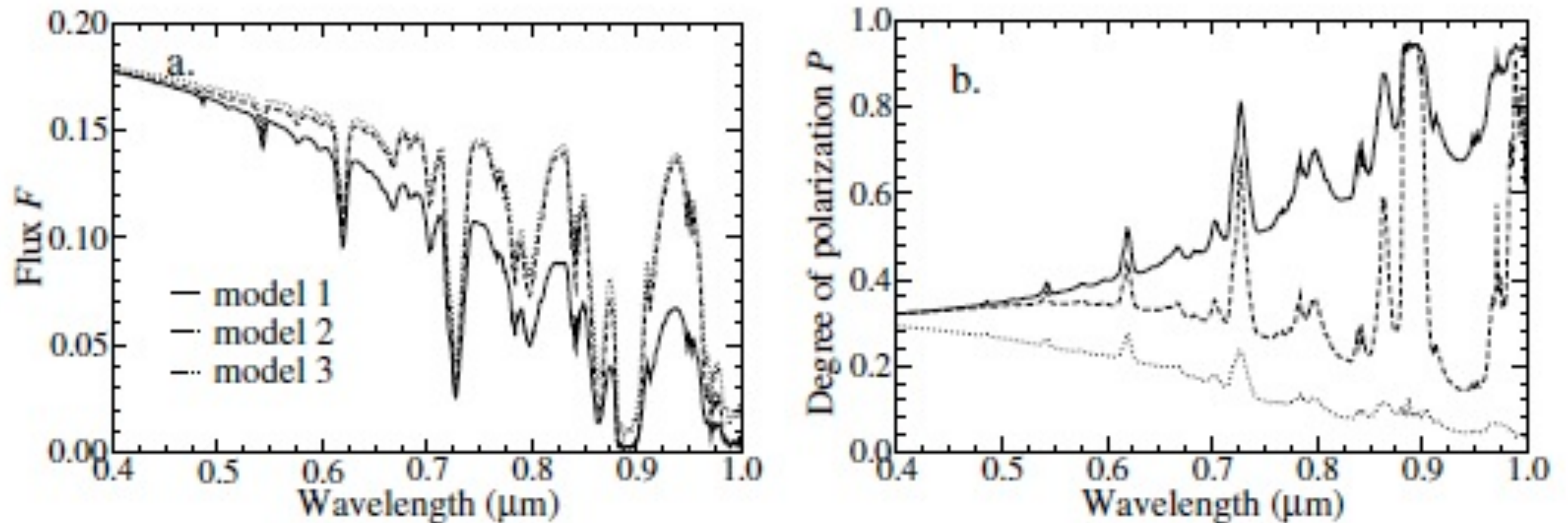


Figure 30. Model and disk-integrated spectrum (left) in the visible and in the infrared (right). Data from the left panel by Woolf *et al.* 2002, reproduced from Tinetti *et al.* 2006. Data from the right panel by Christenson *et al.* 1997, reproduced from Kaltenecker *et al.* 2006).

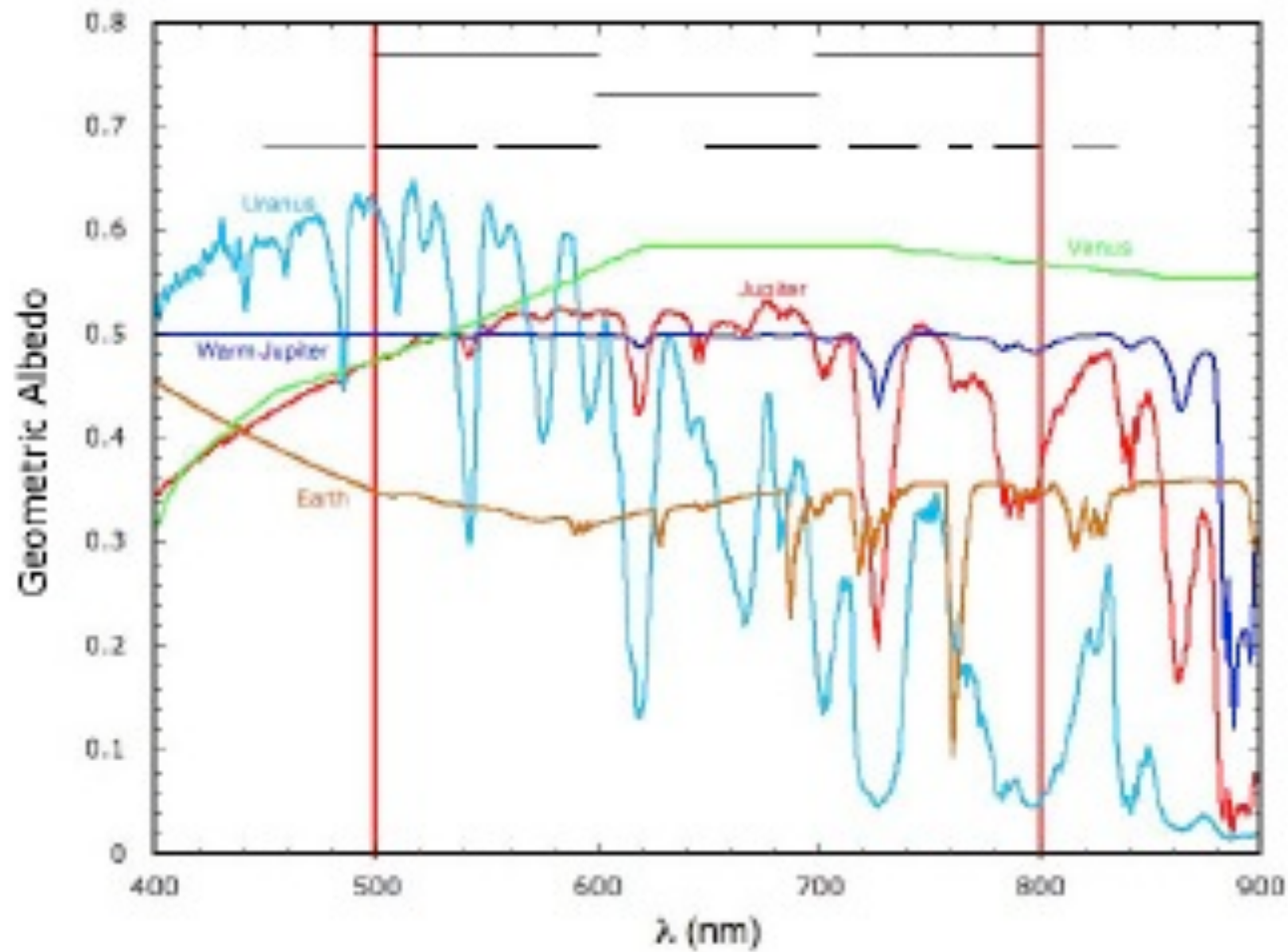


Outer planet spectra, with a methane comparison (Karkoschka 1998)

Planet spectra and polarization



Spectro-polarization is an attractive tool for the identification of companions in reflected starlight. Figures show the calculated spectra and polarization for a mature (cool) EGP at quadrature. Model 1 with no clouds, Model 2 adds tropospheric cloud deck, Model 3 adds stratospheric haze (Stam et al. 2004).



*Sorting out planet types: Filter choices for a coronagraph.
(Marley, Exoplanet Community Report, 2009)*

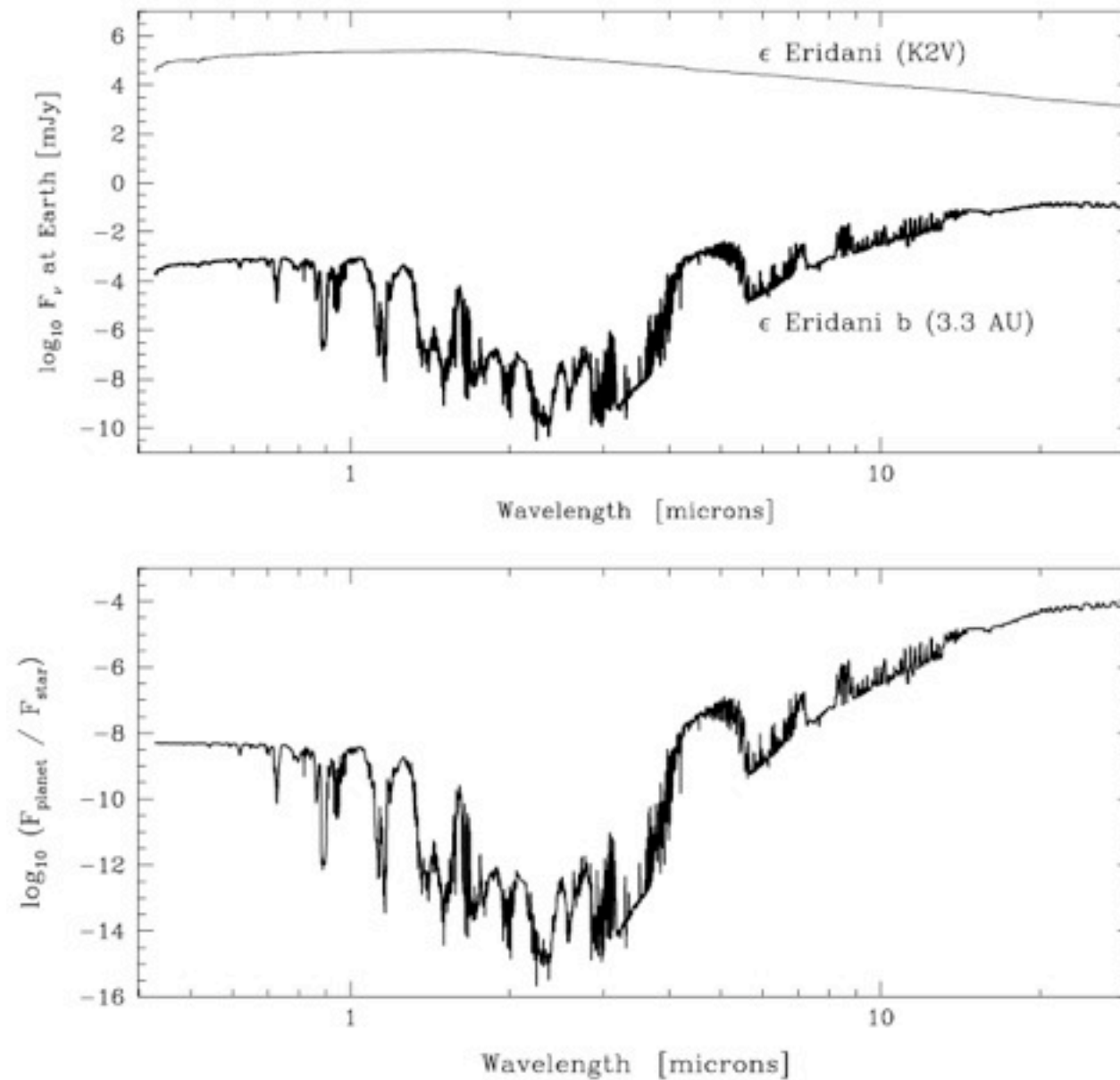
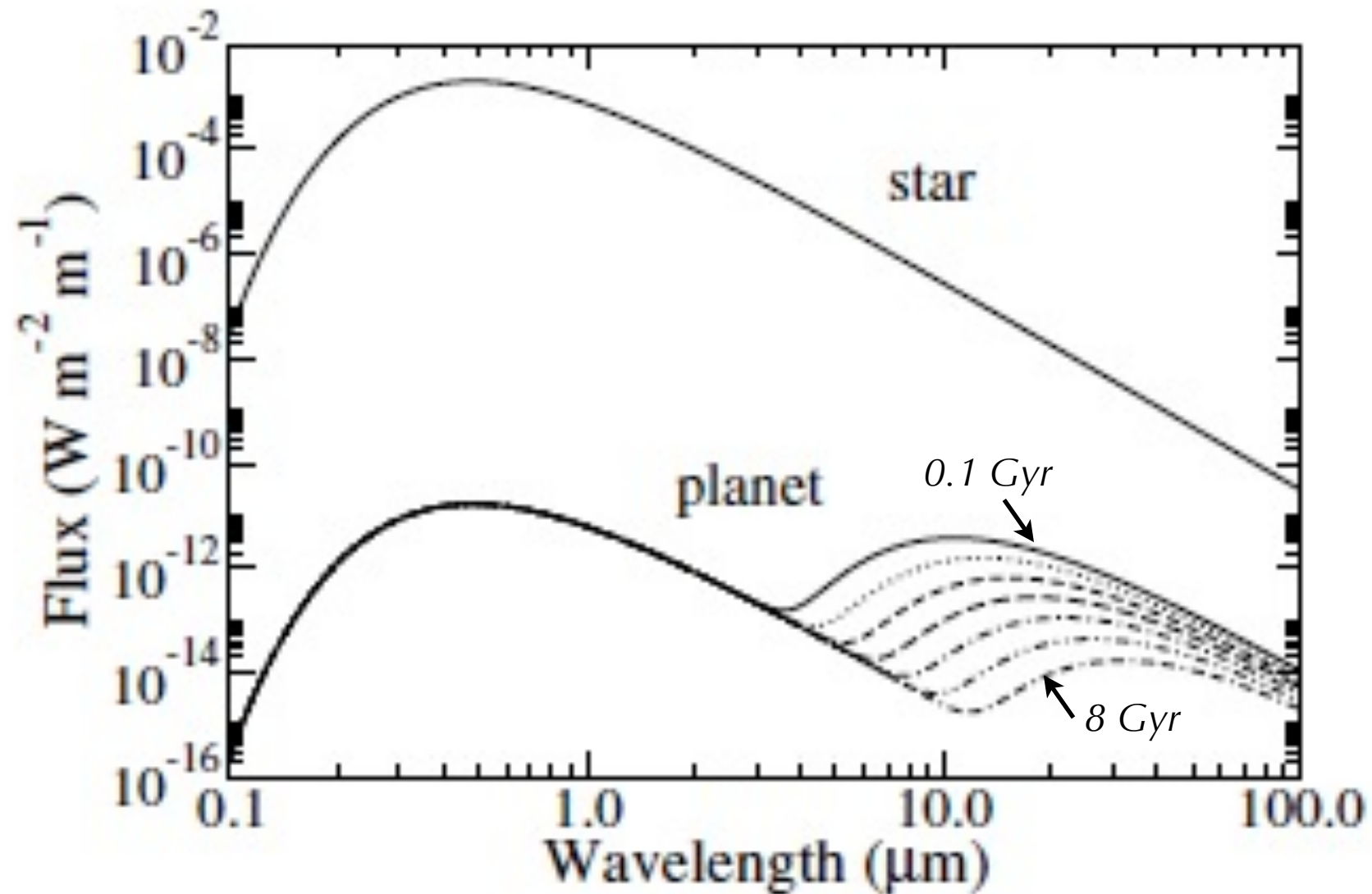


Fig. 35.— *Upper panel*: Model spectrum of ϵ Eri b from 0.4 to 30 μm . ϵ Eri b is a Class II EGP with a water cloud layer near a pressure of 1 bar. For this fiducial model, a cloud particle size distribution peaked at 5 μm is used, and 10% of the available H_2O is assumed to condense. *Lower panel*: Wavelength-dependent planet-to-star flux ratios for ϵ Eri b.

(Sudarsky, Burrows, Hubeny 2003)

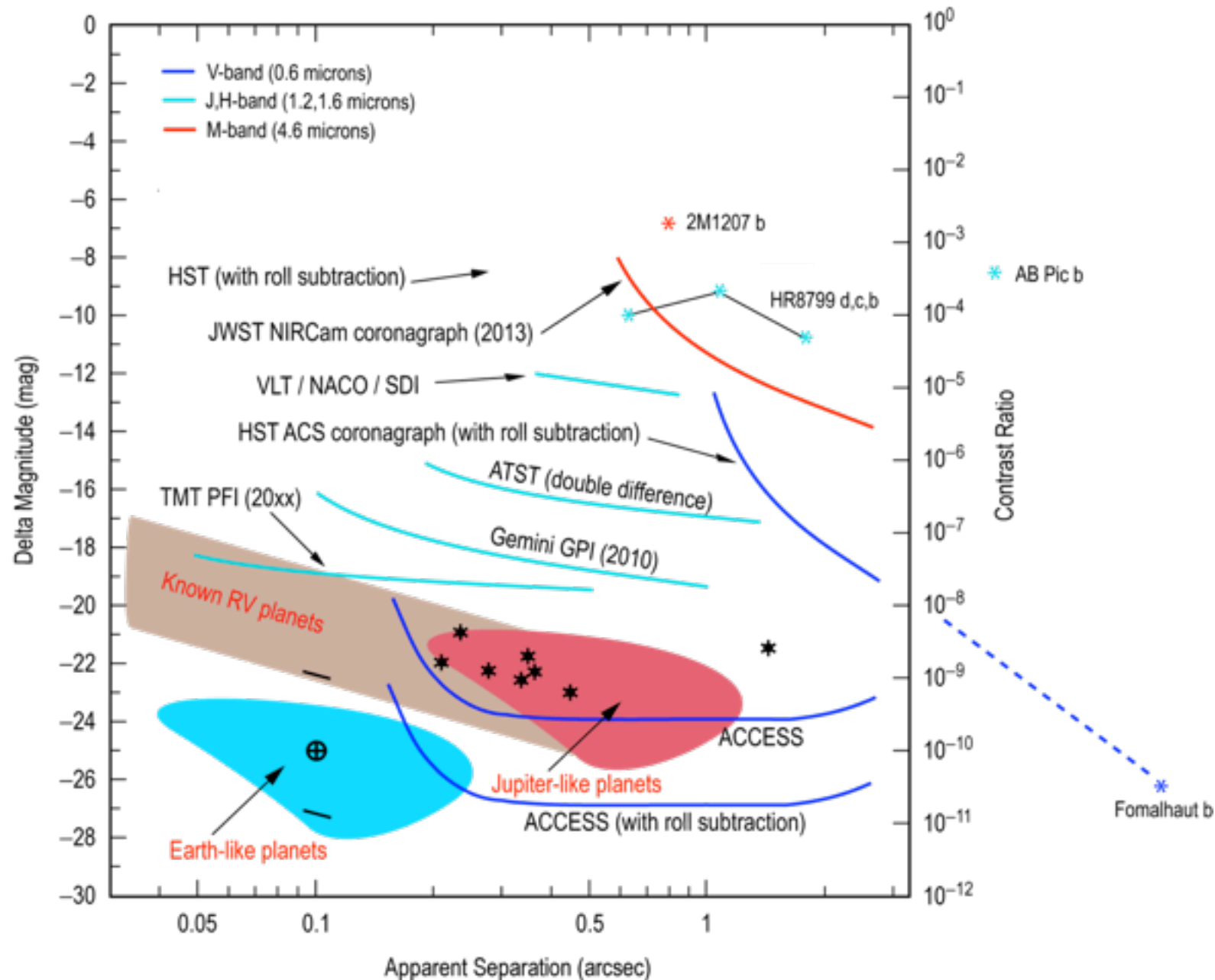
Star & Exosolar Giant Planet Flux



(Stam et al. 2004)

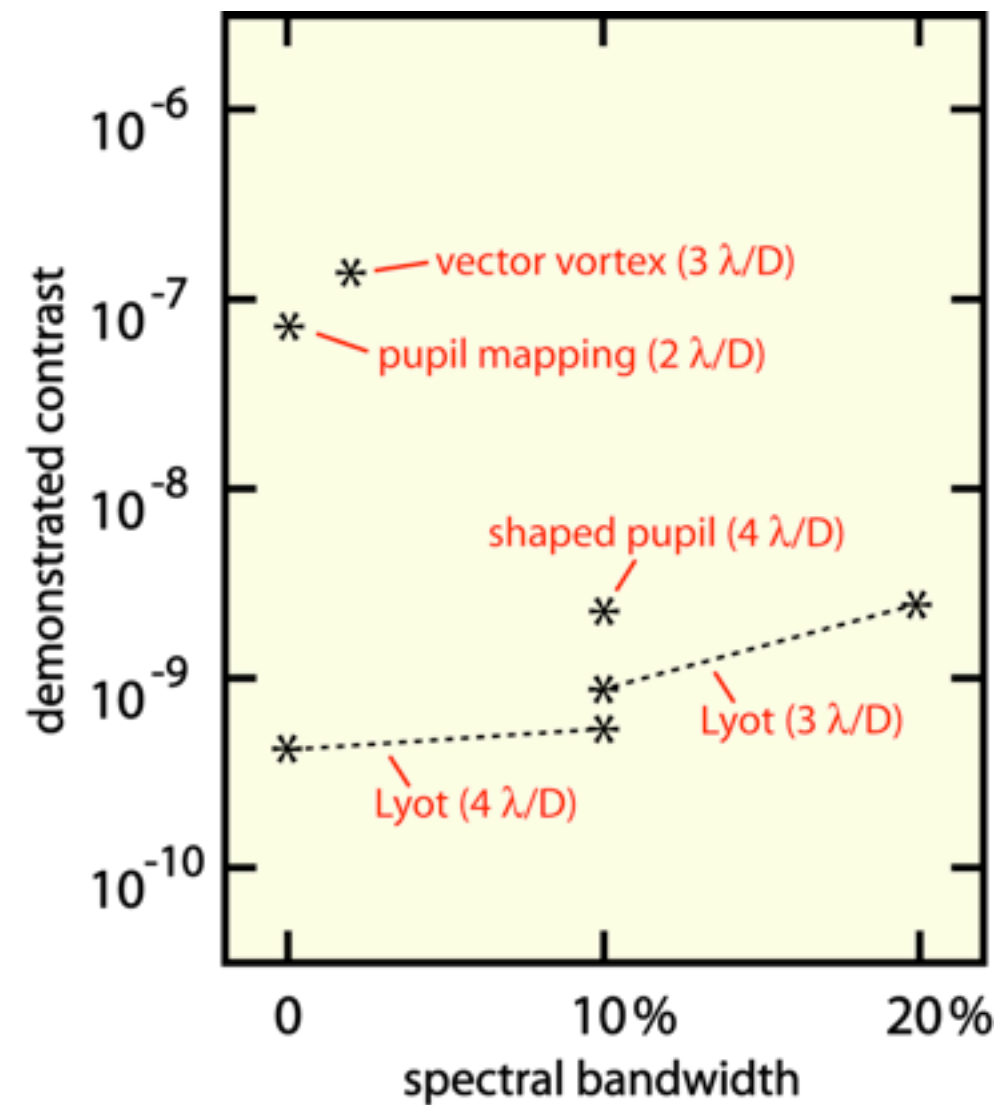
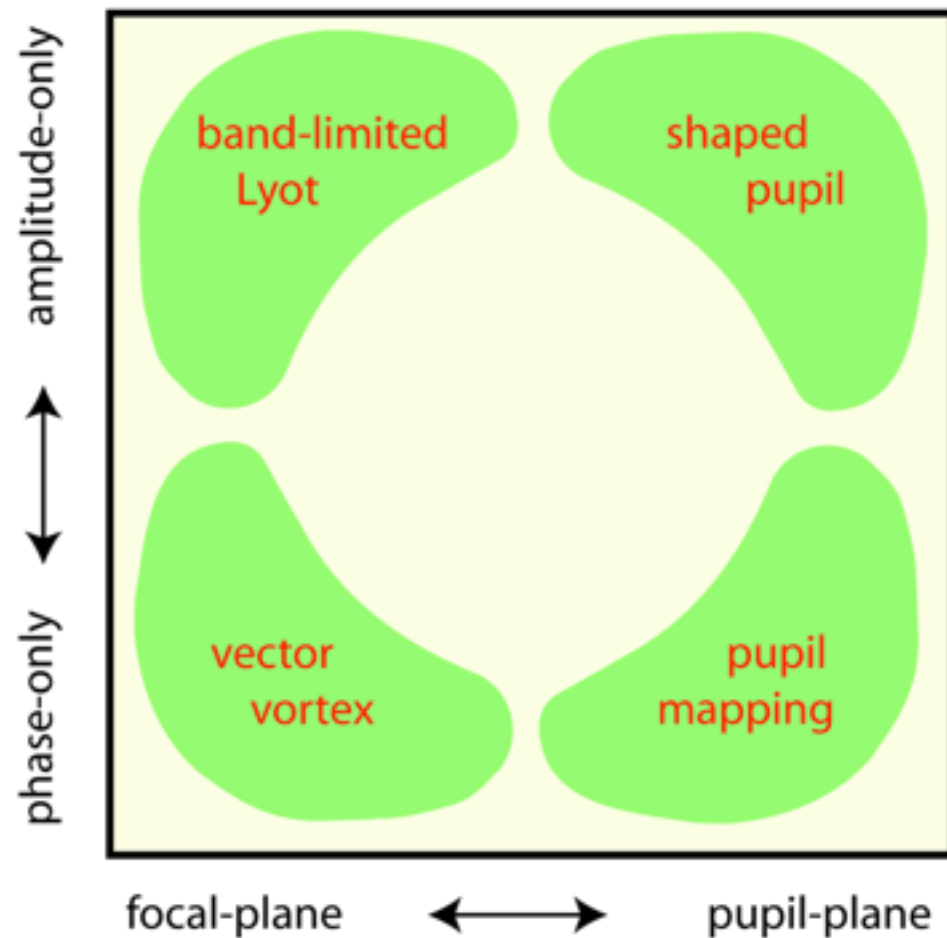
Flux from exo-Jovian planets of various ages.

Coronagraph discovery space



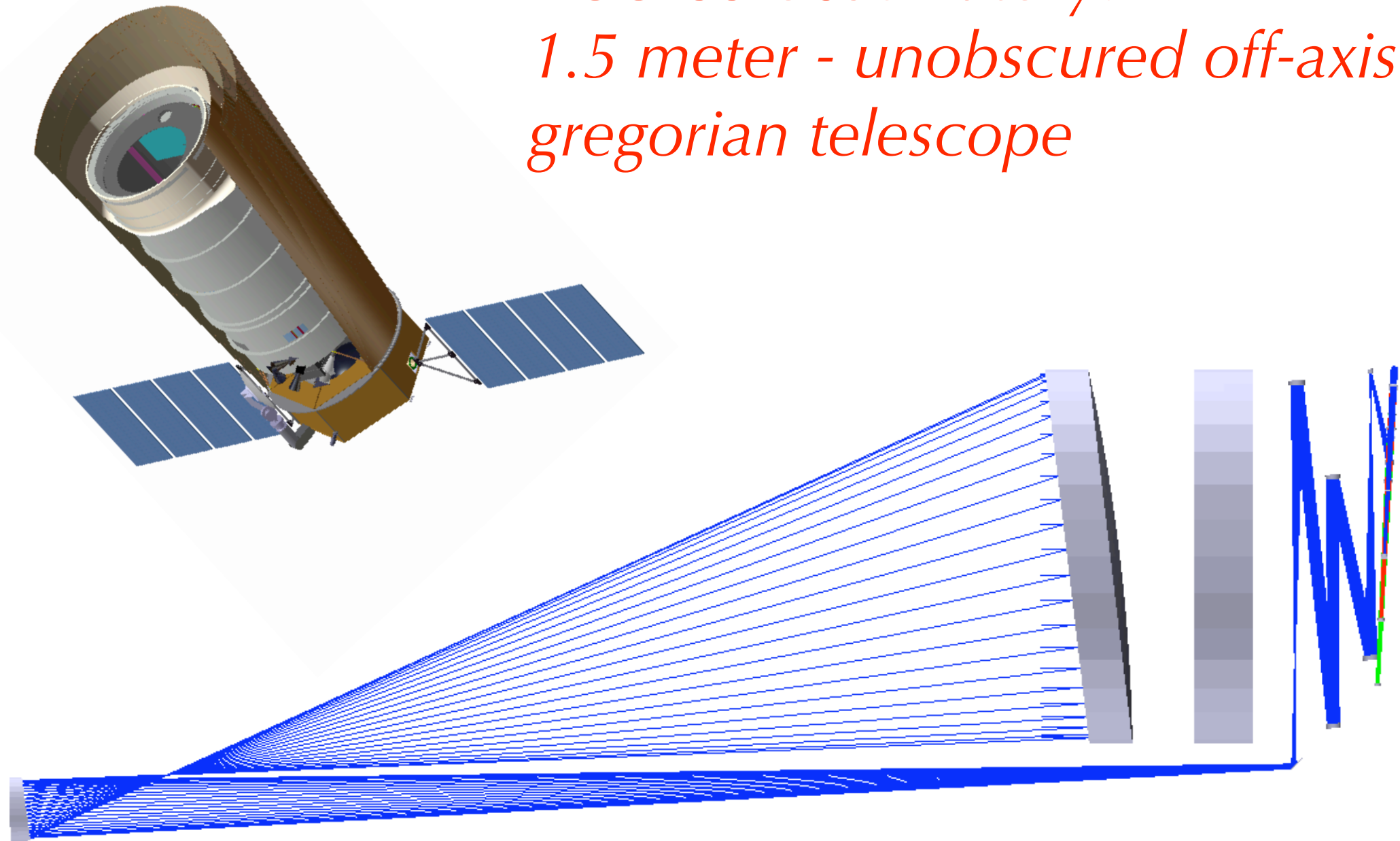
Comparison of detection limits for current, planned, and proposed observatories. The red blob marks the range of 95% confidence limits for detection of a Jupiter-twin orbiting the nearest 100 AFGK stars. The blue blob corresponds to Earth-twins. ACCESS is a representative medium-class 1.5 meter space coronagraph concept.

ACCESS gamut of coronagraph types



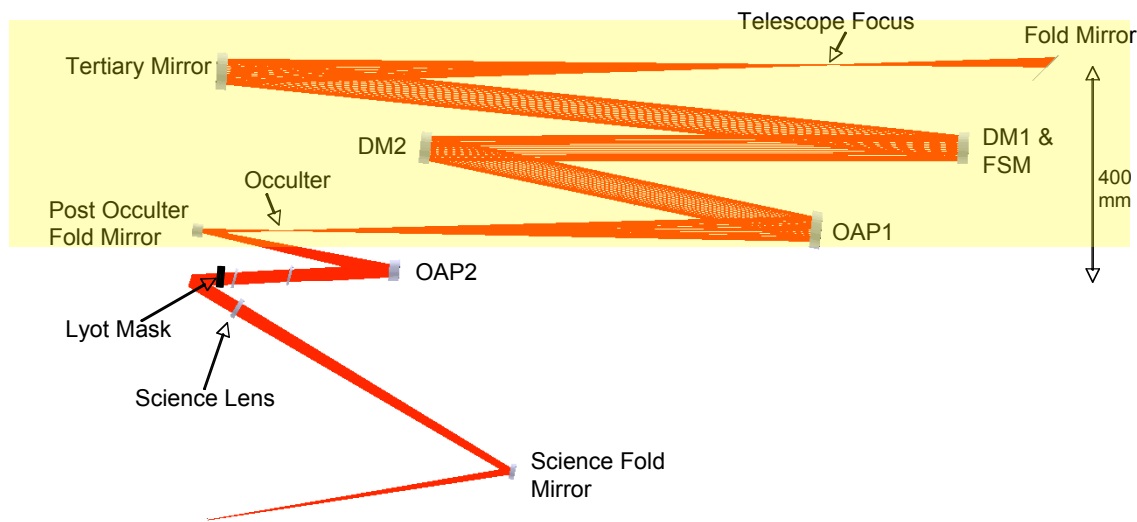
The four major coronagraph types perform starlight rejection with combinations of phase and amplitude elements placed in focal and pupil planes. Best demonstrated laboratory contrast to date (October 2009) for each type are indicated at right, while noting that significant improvements are expected in the coming year as an outcome of active laboratory developments with well-understood technologies.

*ACCESS observatory:
1.5 meter - unobscured off-axis
gregorian telescope*

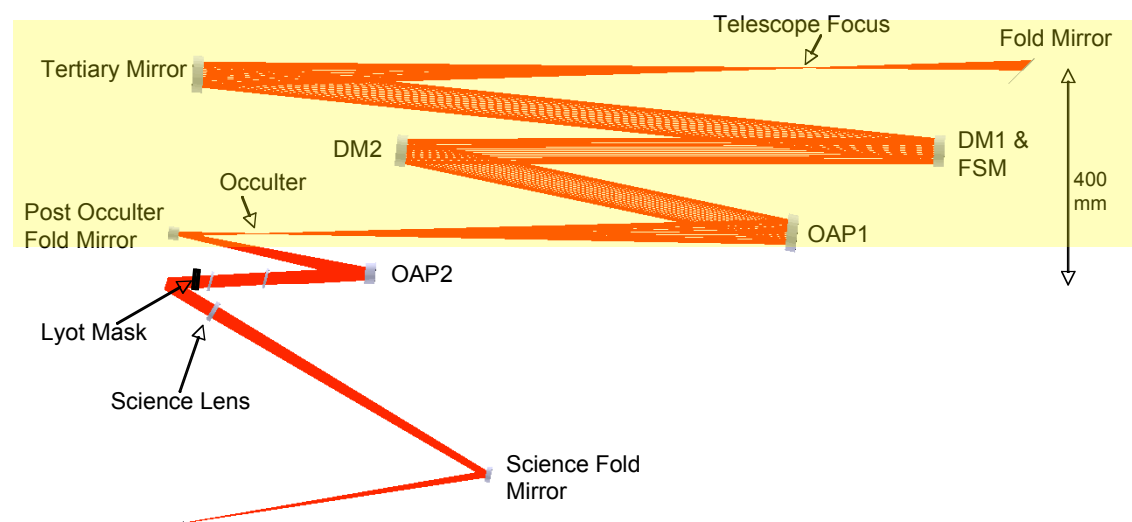


ACCESS compares four major coronagraph types

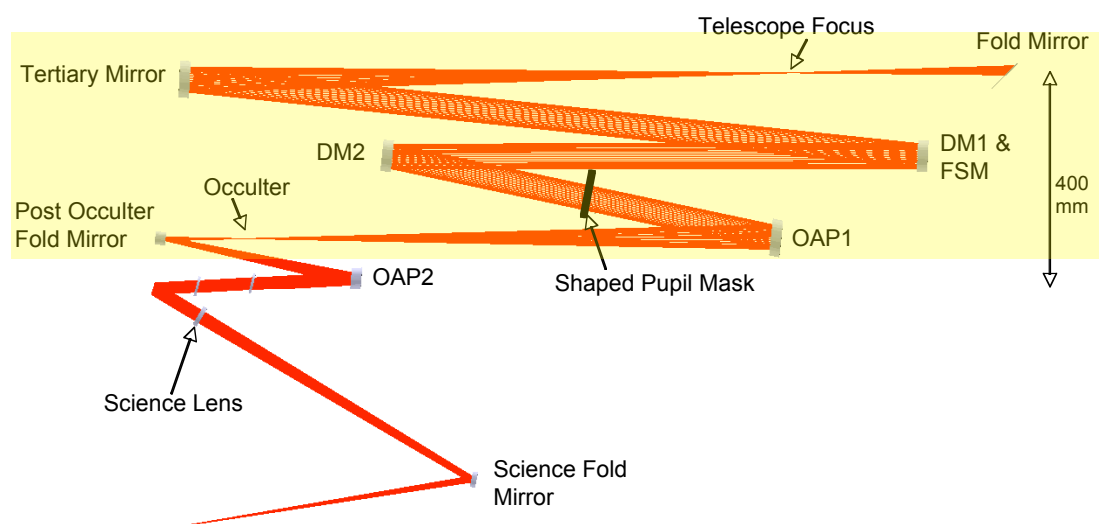
Lyot coronagraph



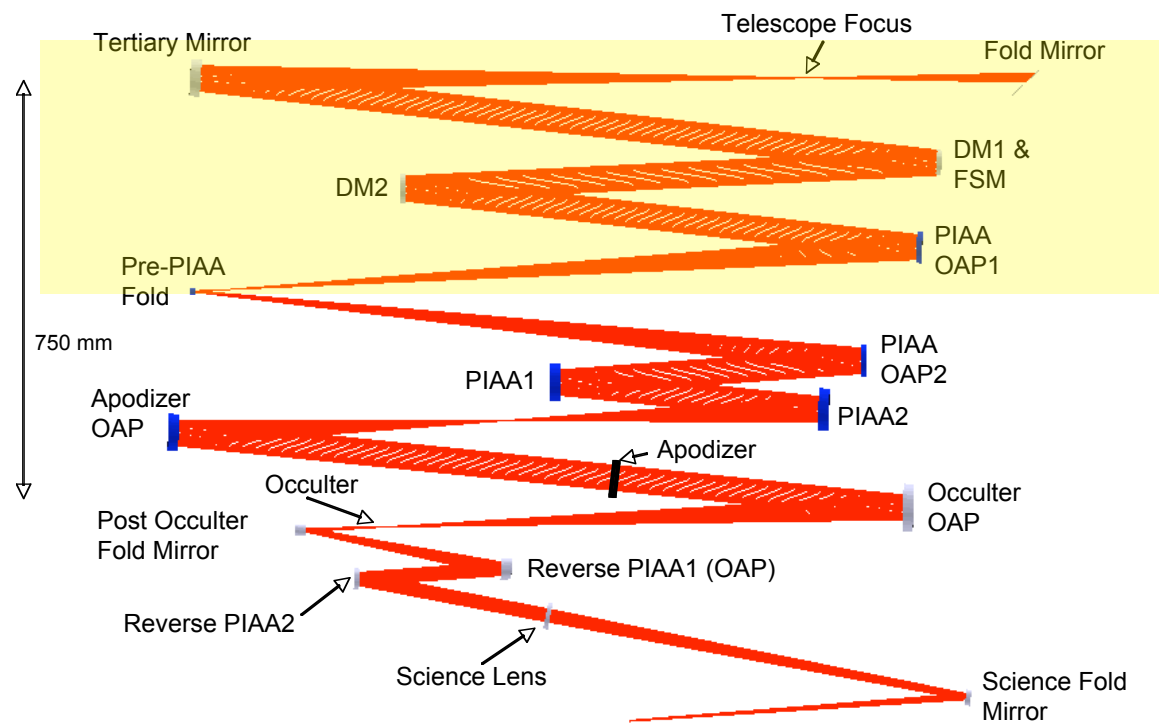
Vortex coronagraph



Shaped pupil coronagraph

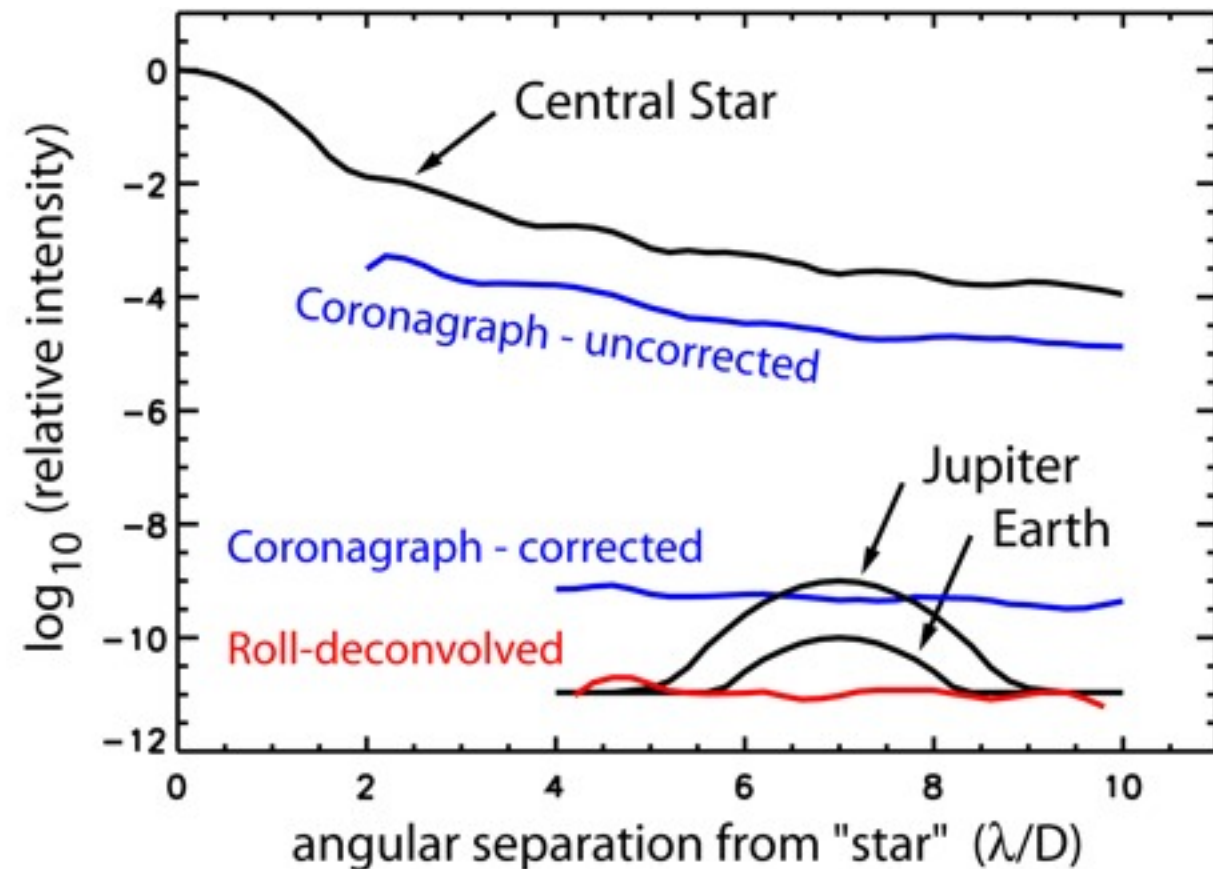
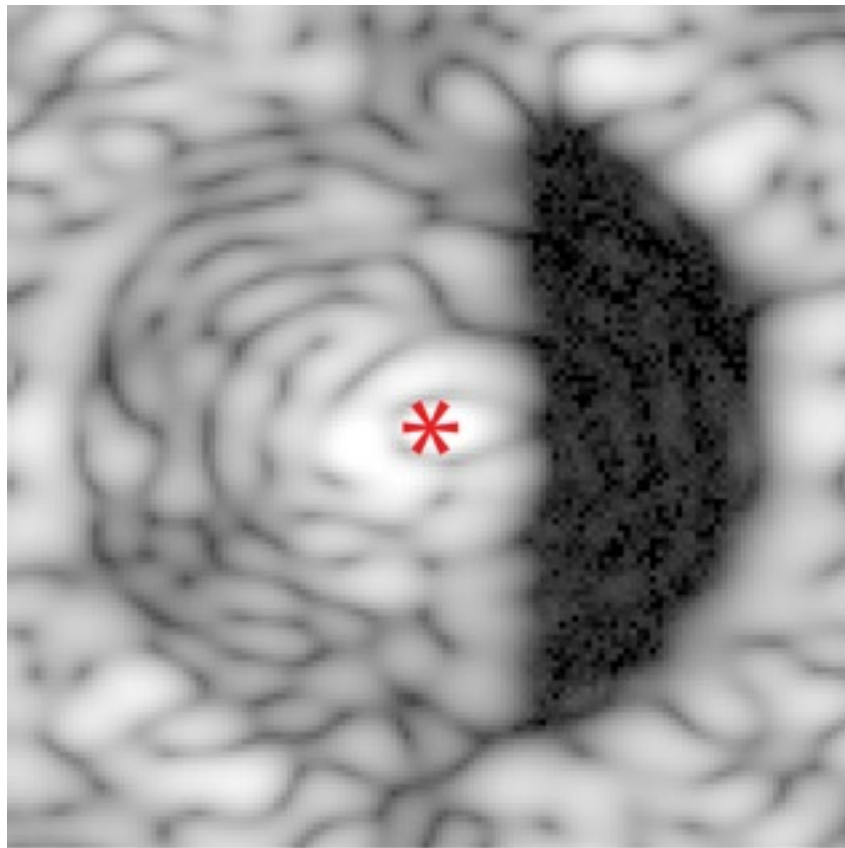


Pupil mapping coronagraph



(Note: highlighted elements, including FSM, DMs, and pointing control system, are common to ALL four coronagraph types)

Laboratory coronagraph contrast and stability demonstrate capability to detect exoplanets



Comparison of azimuthally averaged PSFs of (a) the star, with focal plane mask offset and Lyot stop in place; (b) the coronagraph field with all DM actuators set to equal voltages; (c) the coronagraph with DM set for a dark half-field; and (d) the result of simulated roll deconvolution with the set of 480 consecutive coronagraph images. PSFs of a nominal Earth and Jupiter are also indicated. (Trauger & Traub, *Nature*, 12 April 2007, p771)

Achievable contrast

However, achievable contrast for all (internal) coronagraphs is limited by the residual wavefront errors according to

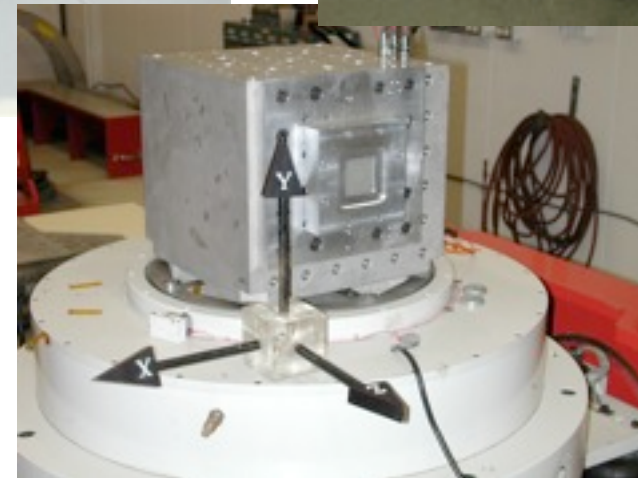
$$C = \pi \left[\frac{\pi \sigma}{N \lambda} \right]^2, \text{ where } N \text{ is the number of}$$

DM actuators across the pupil diameter. A raw contrast of $1e-9$ at 550 nm wavelength requires wavefront errors of order 0.1 nm rms, a level that has been consistently demonstrated in a vacuum laboratory environment for the past four years. Hence the appeal of a space platform. Post-processing of the images, leveraging roll subtractions or other means, will improve the achievable contrast by factors of 10 or more.

Precision deformable mirrors provide wavefront control

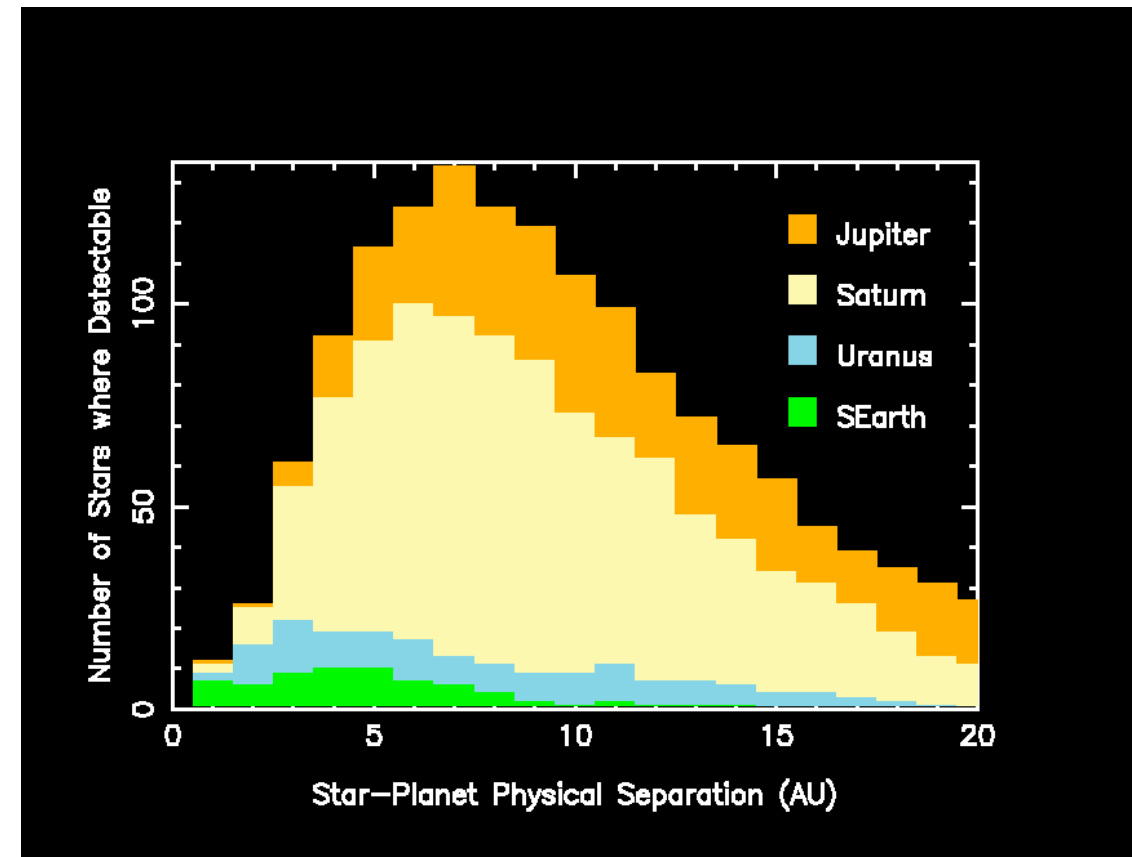
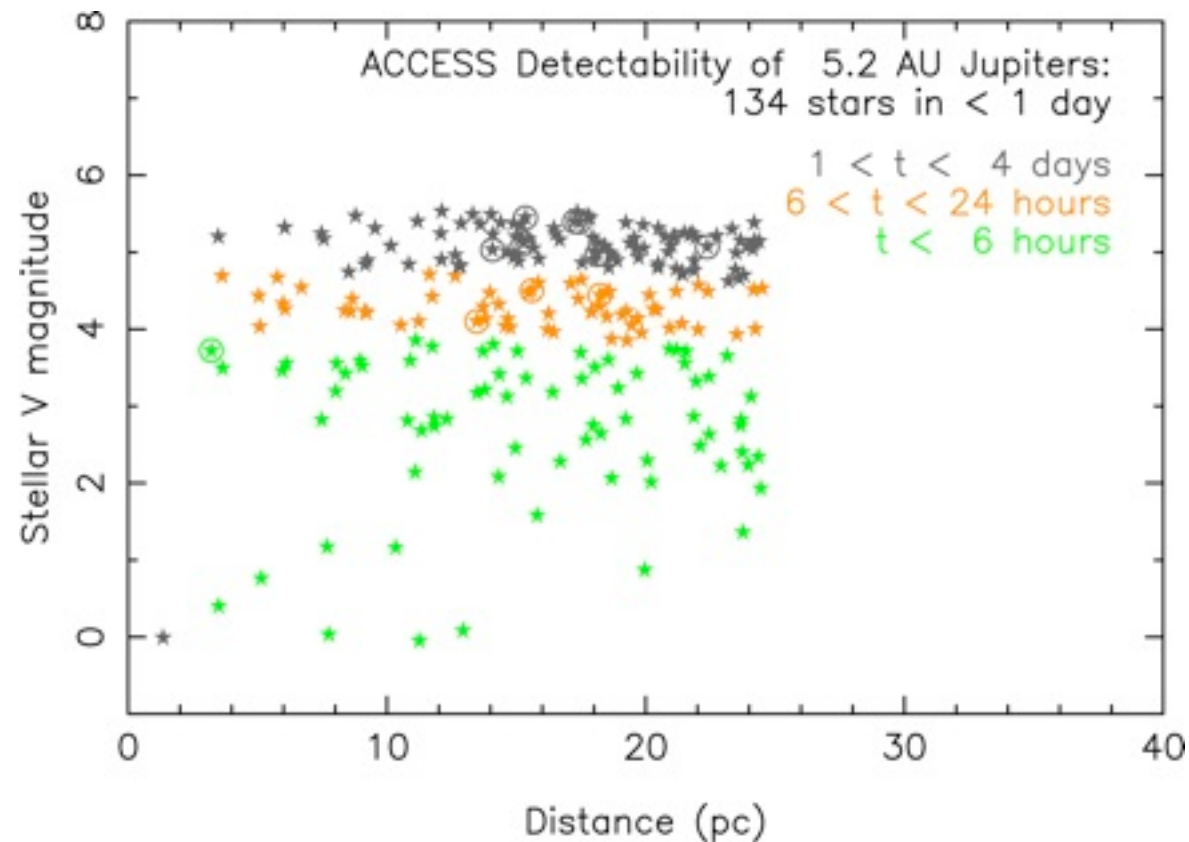


*Evolution of monolithic PMN deformable mirrors:
left to right: 32x32 array, used for all HCIT
milestones to date; 64x64 array to be installed on
HCIT spring 2009; 48x48 array (also shown on
JPL shake table) will be used to demonstrate TRL6
flight-readiness this year.*



Mirror facesheets are fused silica, with surfaces polished nominally to $\lambda/100$ rms. Surface figure (open loop) is settable and stable to 0.01 nm rms over periods of 6 hours or more in a vacuum testbed environment. All DMs were delivered to JPL by Xinetics.

Exoplanet completeness space



Examples of exoplanet search space. At left, a plot of integration times needed to detect Jupiter twins within 45 degrees of elongation from their parent stars, to $S/N = 10$, using the ACCESS Lyot coronagraph with an IWA = $2 \lambda/D$. At right, the number of planets detectable to $S/N = 10$, in integration times of one day or less, using the ACCESS Lyot coronagraph with an IWA = $2.5 \lambda/D$.

Science completeness metric: 2.0, 2.5, and 3.0 λ/D

Table 1: Number of nearby stars that can be surveyed for 5.2 AU Jupiters, IWA 3 I/D

Coronagraph Type	Planet 45° from max elong	Planet 15° from max elong
Lyot	117	175
PIAA	166	278
Vortex	135	204

Table 2: Number of nearby stars that can be surveyed for 5.2 AU Jupiters, IWA 2.5 I/D

Coronagraph Type	Planet 45° from max elong	Planet 15° from max elong
Lyot	153	218
PIAA	178	267
Vortex	154	228

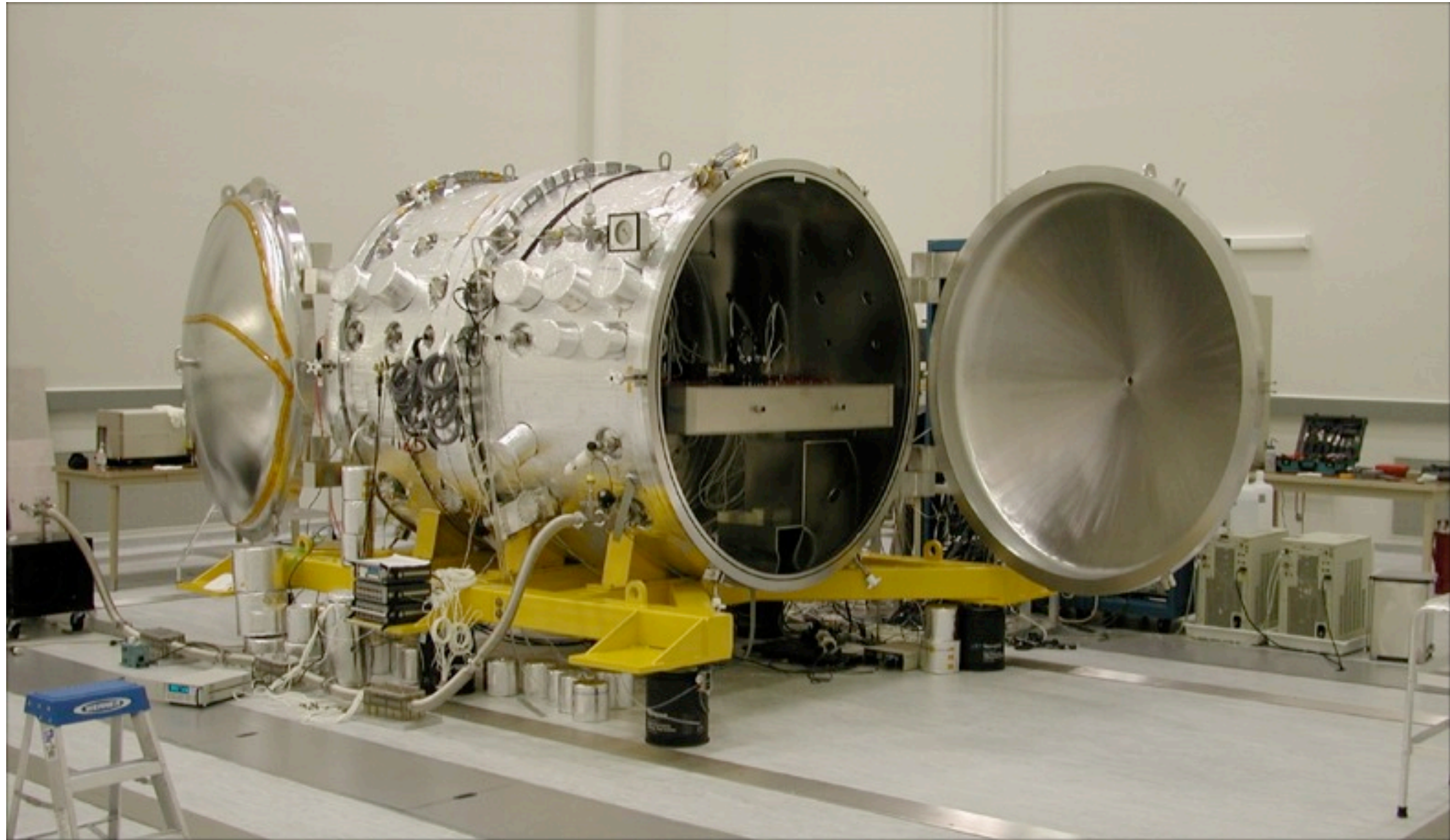
Table 3: Number of nearby stars that can be surveyed for 5.2 AU Jupiters, IWA 2.0 I/D

Coronagraph Type	Planet 45° from max elong	Planet 15° from max elong
Lyot	170	230
Vortex	164	241

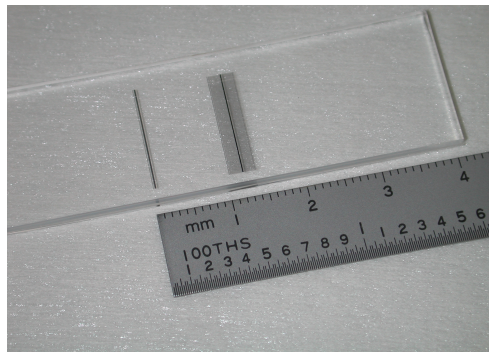
Note: Accurate PIAA wavefront control solution not available for this IWA

Tabulation of the number of nearby stars that could be searched with various ACCESS coronagraphs to the depth of 10-sigma detections of Jupiter twins in each of six visits to the star over a period of 2.5 years. The green-highlighted row is the demonstrated coronagraph state of the art, 3.0 λ/D with the Lyot coronagraph. The blue-highlighted rows represent coronagraph demonstrations that can realistically be achieved this year. Columns for 45 degrees from maximum elongation corresponds to an observational completeness of 50% or more in each visit, approaching 100% after six epochs spread over several years, and for systems with more than one major planet.

*All four coronagraph types have been tested in
JPL's High Contrast Imaging Testbed*

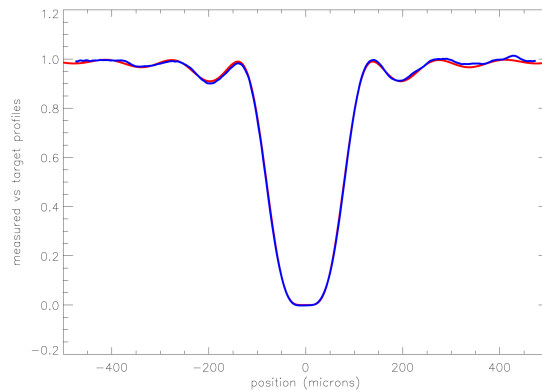


Lyot coronagraph demonstrations on the HCIT



THICKNESS-PROFILED NICKEL MASK

Nickel mask has been vacuum-deposited on a fused silica substrate. Attenuation profile was built up in a number of passes with a computer-controlled moving slit. The same mechanism will be used to superimpose a dielectric phase layer in future work.

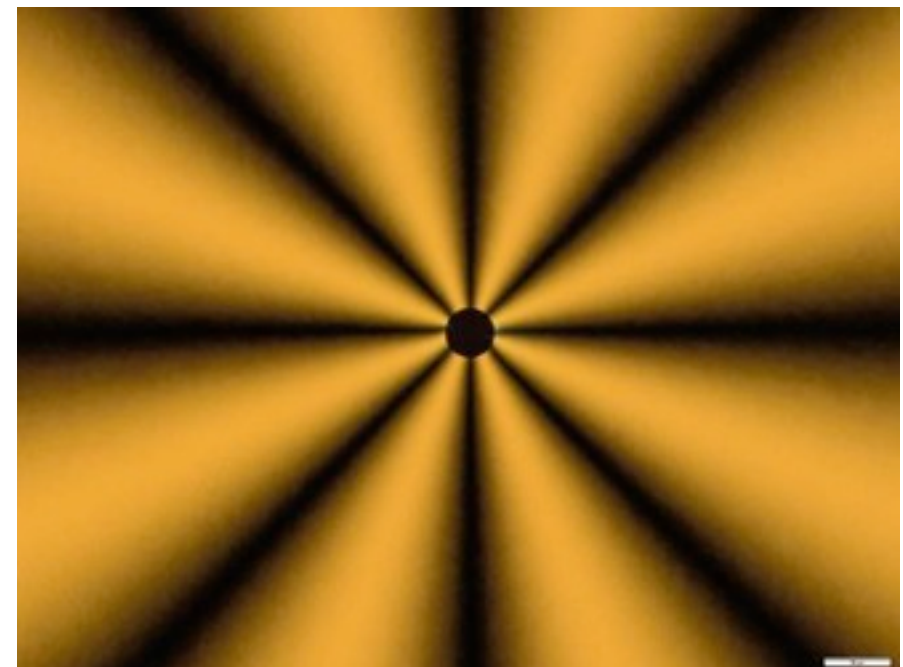


Comparison of the prescribed transmittance profile with the measured profile of the mask pictured at left. Desired profile is the red curve, the measured profile is the blue curve.

Recent contrast demonstrations in the HCIT:
 $IWA = 3 \lambda/D$, 10% bandwidth, $C = 1.2 e-9$
 $IWA = 3 \lambda/D$, 20% BW, $C = 2.7 e-9$
 $IWA = 4 \lambda/D$, 10% BW, $C = 6 e-10$,
with 4th-order metallic or metal+dielectric 4th-order Lyot masks. All masks manufactured at JPL. Narrower ($2.5 \lambda/D$) Lyot masks, and circular masks will be manufactured this year.

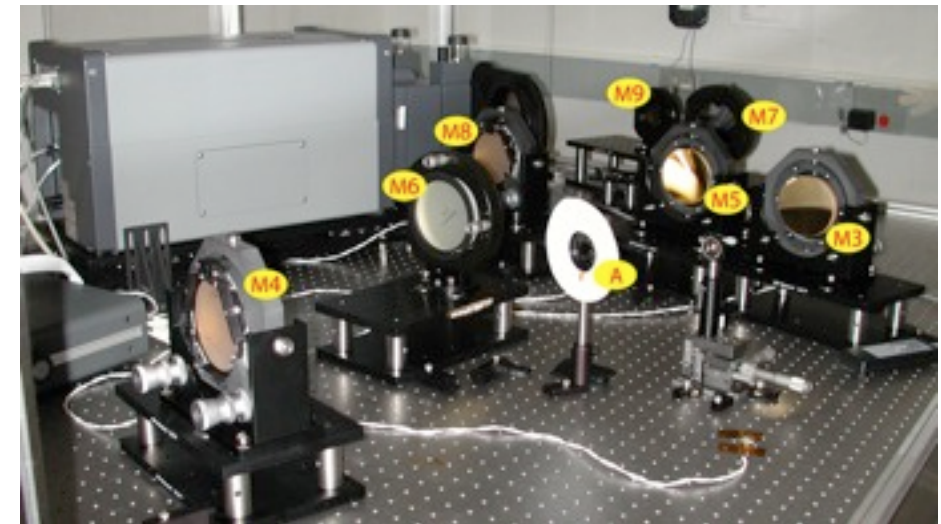
Vector vortex coronagraph mask for HCIT experiments

Recent contrast demonstrations in the HCIT:
 $IWA = 3 \lambda/D$, 2% bandwidth, $C = 2.0 e-7$
with the first-ever charge-4 liquid crystal polymer vortex mask from JDSU (seen at left through crossed polarizers). Close agreement between HCIT performance and models predict that reduction of internal reflections and multilayer achromatization will lead to contrast $\sim 1e-9$ with a 20% bandwidth, to be attempted by the end of this year.

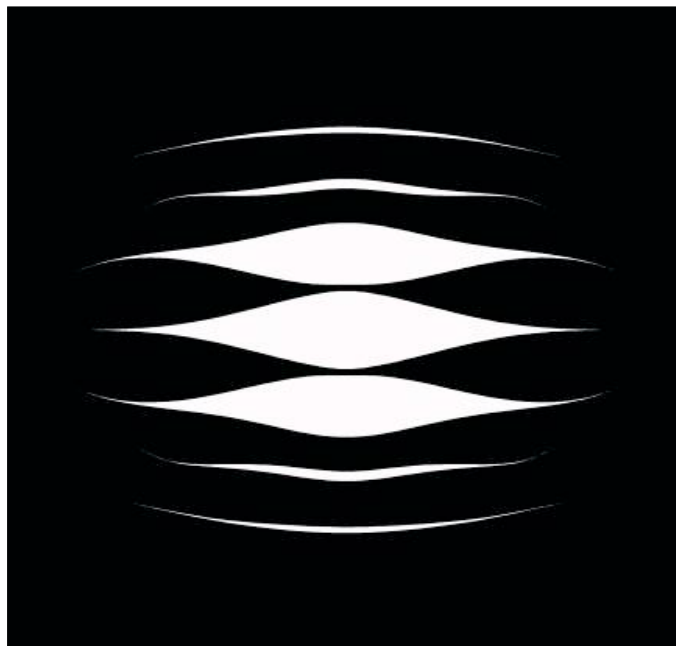


HCIT laboratory setup for pupil mapping demonstrations

To date, the best contrast result for a pupil mapping (PIAA) coronagraph:
 $IWA = 2 \lambda/D$, monochromatic, $C = 7e-8$
has been achieved by Belikov (2009) at NASA/Ames. PIAA experiments continue at both Ames and JPL.



Shaped pupil coronagraph experiments with HCIT



At left, the transmittance profile of a representative shaped pupil apodization (black indicates opaque). This “Ripple 3” design achieved:
 $IWA = 4 \lambda/D$, 10% bandwidth, $C = 2.4 e-9$
on the HCIT (Belikov et al. 2007). Smaller inner working angles are possible with the use of a pair of DMs

Summary

- *Coronagraphs separate the planet photons from starlight, providing an avenue to exoplanet imaging, photometry, spectroscopy, and spectropolarimetry.*
- *Coronagraph architecture is not the fundamental barrier to planet detection: laboratory contrast levels have reached the level needed to detect planets down to earth size, and new methods are progressing.*
- *The critical limitation remains telescope pointing and wavefront control.*
- *The space environment provides an optimal platform for wavefront stability and control.*
- *Suborbital platforms are severely limited by the wavefront errors, not by the coronagraph architecture.*
- *The next order-of-magnitude advance in direct exoplanet imaging will come from improved wavefront knowledge, active/adaptive wavefront control, and methods for post-processing.*

End